

Damping of neutrino oscillations, decoherence and the lengths of neutrino wave packets

Evgeny Akhmedov and Alexei Y. Smirnov

*Max-Planck-Institut für Kernphysik, Saupfercheckweg 1,
69117 Heidelberg, Germany*

E-mail: akhmedov@mpi-hd.mpg.de, smirnov@mpi-hd.mpg.de

ABSTRACT: Spatial separation of the wave packets (WPs) of neutrino mass eigenstates leads to decoherence and damping of neutrino oscillations. Damping can also be caused by finite energy resolution of neutrino detectors or, in the case of experiments with radioactive neutrino sources, by finite width of the emitted neutrino line. We study in detail these two types of damping effects using reactor neutrino experiments and experiments with radioactive ^{51}Cr source as examples. We demonstrate that the effects of decoherence by WP separation can always be incorporated into a modification of the energy resolution function of the detector and so are intimately entangled with it. We estimate for the first time the lengths σ_x of WPs of reactor neutrinos and neutrinos from a radioactive ^{51}Cr source. The obtained values, $\sigma_x = (2 \times 10^{-5} - 1.4 \times 10^{-4})$ cm, are at least six orders of magnitude larger than the currently available experimental lower bounds. We conclude that effects of decoherence by WP separation cannot be probed in reactor and radioactive source experiments.

Contents

1	Introduction	1
2	Separation of wave packets vs. energy averaging	3
2.1	Wave packet approach and the oscillation damping factor	3
2.2	Finite energy resolution and energy averaging in reactor experiments	5
2.3	Radioactive source experiments	6
3	Lengths of neutrino wave packets	9
3.1	Wave packets of reactor (anti)neutrinos	9
3.1.1	Neutrino WPs in the case of delocalized accompanying particles	9
3.1.2	Effects of localization of the decay products	11
3.2	WP lengths and neutrino spectra in radioactive source experiments	13
4	Discussion	16

1 Introduction

Recently, there has been an increased interest in studying the manifestations of the wave packet (WP) nature of neutrinos in neutrino oscillations. In a number of papers the possibility of probing quantum decoherence effects due to the separation of the WPs of different neutrino mass eigenstates composing an emitted flavour-state neutrino was discussed. In particular, possible manifestations of neutrino WP separation in reactor experiments [1–5] and experiments with radioactive neutrino sources [5] have been investigated (for earlier and related discussions, including those for other neutrino experiments, see e.g. [6–14]).

In [1] the Daya Bay collaboration has analyzed their reactor neutrino data taking into account possible decoherence effects due to the finite momentum spread σ_p of the neutrino WPs and treating σ_p/p , along with $\sin^2 2\theta_{13}$ and Δm_{32}^2 , as a free parameter. The relative momentum uncertainty was thus assumed to be momentum-independent. Their analysis produced the constraint $\sigma_p/p < 0.23$ at 95% C.L. Note that for typical momenta of reactor neutrinos $p \simeq 3$ MeV this approximately corresponds to the length of the neutrino WP $\sigma_x \simeq 1/\sigma_p \gtrsim 2.8 \times 10^{-11}$ cm.

The authors of [2, 3] have carried out a similar analysis of the data of the Daya Bay, RENO and in [3] also of the KamLAND reactor neutrino experiments, but using the length of neutrino WP σ_x rather than σ_p/p as a fit parameter. From their combined fit they found the lower bound

$$\sigma_x > 2.1 \times 10^{-11} \text{ cm (90\% C.L.)}. \quad (1.1)$$

In [2] also the sensitivity of the future medium-baseline JUNO experiment to decoherence effects due to neutrino WPs separation was considered. It was found that JUNO would be

able to improve the bound of eq. (1.1) by an order of magnitude. The JUNO collaboration itself, following the analysis of [6], has studied the expected sensitivity of their experiment to various mechanisms of damping of neutrino oscillations, including damping due to neutrino WP separation [4]. They concluded that JUNO should be able to set the limits $\sigma_p/p < 1.04 \times 10^{-2}$ and $\sigma_x > 2.3 \times 10^{-10}$ cm, both at 95% C.L.

In [5] possible effects of decoherence by neutrino WP separation on the searches for oscillations of ν_e and $\bar{\nu}_e$ to sterile neutrinos ν_s were considered. The authors discussed the tension between the results of short-baseline reactor experiments, which put constraints on $\nu_e \rightarrow \nu_s$ oscillations, and the BEST radioactive neutrino source experiment [15–17], which claimed a positive signal. Assuming that the actual value of σ_x coincides with the lower bound 2.1×10^{-11} cm given in eq. (1.1), the authors argued that, due to possible damping effects, the results of BEST and of the reactor experiments can be reconciled with each other. They, however, did not take into account the effects of finite energy resolution of the detectors, which play a crucial role in the analyses of the oscillation damping. We shall discuss ref. [5] in more detail in section 4.

How does the separation of neutrino WPs occur? Neutrinos of different mass m_i propagate with different group velocities $v_{gi} = \partial E_i / \partial p_i$, and for ultra-relativistic or almost degenerate in mass neutrinos their difference satisfies

$$\frac{\Delta v_g}{v_g} \simeq \frac{\Delta m^2}{2E^2}. \quad (1.2)$$

Because of this velocity difference and of the finite lengths of the neutrino WPs, the overlap of the WPs of different neutrino mass eigenstates composing an emitted neutrino flavor state will decrease with time. If neutrinos propagate sufficiently long distance, these WPs will completely separate.

Neutrino oscillations are a quantum mechanical (QM) interference phenomenon; separation of the WPs of different neutrino mass eigenstates will suppress their interference in the oscillation probability and therefore will damp the oscillations. Requiring the spatial separation of the WPs to be smaller than the length of their WPs, one finds the constraint on the distance L traveled by the neutrinos:

$$L < L_{\text{coh}} \equiv \frac{v_g}{\Delta v_g} \sigma_x, \quad (1.3)$$

where $\sigma_x \simeq v_g / \sigma_E$ is the length of the neutrino WP. Here σ_E is the intrinsic QM uncertainty of the neutrino energy related to the localization of its production and detection processes. Taking into account eq. (1.2), for ultra-relativistic neutrinos condition (1.3) yields

$$\frac{\sigma_E}{E} < \frac{1}{2\pi} \frac{l_{\text{osc}}}{L}, \quad (1.4)$$

where $l_{\text{osc}} \equiv \frac{4\pi E}{\Delta m^2}$ is the neutrino oscillation length.

Quantum decoherence due to WP separation is not the only possible reason for damping of neutrino oscillations. The damping may also occur due to the averaging over the baseline L related to the uncertainties of the coordinates of the neutrino emission and

absorption points, both due to the finite spatial extensions of the elementary production and detection processes and, more importantly, due to the macroscopic sizes of the neutrino source and detector. For neutrino oscillations to be observable, the corresponding averaging regions should be small compared to the neutrino oscillation length, i.e. neutrino production and detection should be sufficiently well localized.

There is yet another possible source of damping of neutrino oscillations: finite energy resolution of the detector δ_E . The experiment will only be able to see the oscillations if the oscillation phase $\phi(E) = \frac{\Delta m^2}{2E}L$ varies little over the energy interval δ_E . Requiring that $|\phi(E) - \phi(E + \delta_E)| < 1$, we find that δ_E must satisfy the inequality

$$\frac{\delta_E}{E} < \frac{1}{2\pi} \frac{l_{osc}}{L}. \quad (1.5)$$

Note that this condition coincides with that in eq. (1.4) with σ_E replaced by δ_E . Additional damping effects can be related to energy binning of the data.

Clearly, averaging over L and E , inherent in any neutrino oscillation experiment, may damp neutrino oscillations and thus mimic quantum decoherence by WP separation. It is therefore mandatory to carefully examine these averaging effects when trying to probe experimentally decoherence due to the WP nature of neutrinos. In the present paper we consider in detail the damping of neutrino oscillations due to decoherence by WP separation and due to energy averaging related to finite experimental energy resolution. We study the entanglement of these two effects for reactor neutrino experiments and experiments with radioactive neutrino sources, though our results have broader applicability. We also estimate the spatial lengths of neutrino WPs in reactor and source experiments and the corresponding intrinsic QM neutrino energy uncertainties. To the best of our knowledge, these are the first consistent estimates of these quantities.

2 Separation of wave packets vs. energy averaging

2.1 Wave packet approach and the oscillation damping factor

In the WP approach, the probability of $\nu_\alpha \rightarrow \nu_\beta$ oscillations in vacuum can be written in the following form (see e.g. [19]):

$$P_{\alpha\beta}(\bar{E}, L) = \sum_{i,k} U_{\alpha i}^* U_{\beta i} U_{\alpha k} U_{\beta k}^* I_{ik}(\bar{E}, L). \quad (2.1)$$

Here L is the baseline and U is the leptonic mixing matrix. The quantity $I_{ik}(\bar{E}, L)$ can be written as [19]

$$I_{ik}(\bar{E}, L) = \int dE |f(E, \bar{E})|^2 e^{-i \frac{\Delta m_{ik}^2}{2E} L}. \quad (2.2)$$

Here

$$f(E, \bar{E}) \equiv f_S(E) f_D^*(E), \quad (2.3)$$

where $f_S(E)$ and $f_D(E)$ are the WPs of the produced and detected neutrinos in energy representation (i.e. the amplitudes of the corresponding energy distributions) and \bar{E} is the

mean energy of the neutrino WP. The quantity $f(E, \bar{E})$ is normalized according to

$$\int dE |f(E, \bar{E})|^2 = 1, \quad (2.4)$$

which gives $I_{ii}(\bar{E}, L) = 1$. The mean energy is defined as $\bar{E} = \int dE E |f(E, \bar{E})|^2$. The function $f(E, \bar{E})$ is an effective neutrino WP in energy space, which takes the quantum nature of both neutrino production and detection into account [19]. The energy distribution amplitudes $f_S(E)$ and $f_D(E)$ have peaks of widths σ_E^S and σ_E^D , respectively. As $f(E, \bar{E})$ is the product of $f_S(E)$ and $f_D(E)$, it has a peak of width $\sigma_E \simeq \min\{\sigma_E^S, \sigma_E^D\}$ with maximum at or near \bar{E} . The quantity $I_{ik}(\bar{E}, L)$ depends on the oscillation phase and on the degree of overlap of the WPs of different neutrino mass eigenstates in momentum and coordinate spaces and thus encodes possible WP-related quantum decoherence effects.

In the present paper we assume that the microscopic localization conditions for neutrino production and detection are fulfilled, i.e. the corresponding averaging over L can be neglected. For elementary neutrino production and detection processes these localization conditions require [18–22]

$$\frac{\Delta m_{ik}^2}{2E} \ll \sigma_E. \quad (2.5)$$

When deriving eqs. (2.2) and (2.3) from the general expressions given in [19], we assumed this condition to be satisfied.¹ We also found it convenient to go from the usual integration over momentum to integration over energy. It should be stressed, however, that the same result could be obtained using coordinate-space neutrino WPs [19].

It is convenient to rewrite the expression for $I_{ik}(\bar{E}, L)$ by pulling the phase factor $\exp(-i\frac{\Delta m_{ik}^2}{2E}L)$ taken at $E = \bar{E}$ out of the integral in eq. (2.2). This yields

$$I_{ik}(\bar{E}, L) = \exp\left(-i\frac{\Delta m_{ik}^2}{2\bar{E}}L\right) D_{ik}(\bar{E}, L) \quad (2.6)$$

with

$$D_{ik}(\bar{E}, L) \simeq \int dE |f(E, \bar{E})|^2 e^{i\frac{\Delta m_{ik}^2}{2\bar{E}^2}(E-\bar{E})L}. \quad (2.7)$$

From the fact that $|f(E, \bar{E})|^2$ has a peak at or near \bar{E} of width σ_E it follows that the main contribution to the integral defining $D_{ik}(\bar{E}, L)$ comes from the region $|E - \bar{E}| \lesssim \sigma_E$. It is then easy to see that for

$$L \ll L_{\text{coh}, ik} \equiv \frac{2\bar{E}^2}{\Delta m_{ik}^2} \sigma_E^{-1} \simeq \frac{2\bar{E}^2}{\Delta m_{ik}^2} \sigma_x \quad (2.8)$$

(which corresponds to the absence of WP separation) one has $D_{ik}(\bar{E}, L) = 1$. Eqs. (2.6) and (2.1) then yield the standard master formula for neutrino oscillations in vacuum: $P_{\alpha\beta}(\bar{E}, L) = P_{\alpha\beta}^0(\bar{E}, L)$, where

$$P_{\alpha\beta}^0(E, L) \equiv \sum_{i,k} U_{\alpha i}^* U_{\beta i} U_{\alpha k} U_{\beta k}^* e^{-i\frac{\Delta m_{ik}^2}{2E}L}. \quad (2.9)$$

¹If this condition were not met, the arguments of $f_S(E, \bar{E})$ and $f_D(E, \bar{E})$ in eq. (2.3) would differ by $\Delta m_{ik}^2/2E$, and the oscillations would be damped.

In the opposite case, $L \gg L_{\text{coh},ik}$ (complete decoherence by WP separation), the integrand of eq. (2.6) contains a fast oscillating phase factor which suppresses the quantities $D_{ik}(\bar{E}, L)$ with $i \neq k$. This gives $D_{ik}(\bar{E}, L) = \delta_{ik}$, and eq. (2.1) yields

$$P_{\alpha\beta}(\bar{E}, L) = \sum_i |U_{\alpha i}|^2 |U_{\beta i}|^2, \quad (2.10)$$

i.e. the oscillations are fully damped. The quantity $D_{ik}(\bar{E}, L)$ with $i \neq k$ is thus the oscillation damping factor. Note that the fully decoherent result (2.10) would also follow from the standard oscillation probability (2.9) upon averaging of all the oscillatory terms.

For illustration, we consider the energy-space neutrino WP of Gaussian form:

$$|f(E, \bar{E})|^2 = \frac{1}{\sqrt{2\pi}\sigma_E} e^{-\frac{(\bar{E}-E)^2}{2\sigma_E^2}}. \quad (2.11)$$

Substituting this into eq. (2.7), from eqs. (2.1) and (2.6) we find

$$P_{\alpha\beta}(\bar{E}, L) = \sum_{i,k} U_{\alpha i}^* U_{\beta i} U_{\alpha k} U_{\beta k}^* \exp\left(-i \frac{\Delta m_{ik}^2 L}{2\bar{E}}\right) D_{ik}(\bar{E}, L), \quad (2.12)$$

where

$$D_{ik}(\bar{E}, L) = e^{-\frac{1}{2} \left(\frac{L}{L_{\text{coh},ik}}\right)^2} \quad (2.13)$$

is the Gaussian the damping factor often used in the literature on neutrino oscillations.

2.2 Finite energy resolution and energy averaging in reactor experiments

The number of neutrino events per unit time in a neutrino experiment can be written as

$$N(E_r) = \mathcal{N} \int d\bar{E} \phi_\alpha(\bar{E}) P_{\alpha\beta}(\bar{E}, L) \sigma_\beta(\bar{E}) R(E_r, \bar{E}), \quad (2.14)$$

where \mathcal{N} is the number of the target particles in the detector, \bar{E} is the discussed above mean energy of the neutrino WPs, E_r is the reconstructed neutrino energy, $\phi_\alpha(\bar{E})$ is the flux of the neutrinos, initially produced as ν_α , impinging on the detector, $\sigma_\beta(\bar{E})$ is the cross section of detection of ν_β and $R(E_r, \bar{E})$ is the energy resolution function of the detector. The oscillation probability $P_{\alpha\beta}(\bar{E}, L)$ contains a damping factor which takes into account possible effect of decoherence by WP separation. For reactor experiments, $\alpha = \beta = e$, but we want to keep our discussion more general at this point, so that it also apply to other beam experiments.

The oscillation probability (2.1) with $I_{ik}(\bar{E}, L)$ from eq. (2.2) can be written as

$$P_{\alpha\beta}(\bar{E}, L) = \int dE |f(E, \bar{E})|^2 P_{\alpha\beta}^0(E, L), \quad (2.15)$$

where $P_{\alpha\beta}^0(E, L)$ is given in eq. (2.9). Substituting (2.15) into (2.14) and changing the order of integrations, we obtain

$$N(E_r) = \mathcal{N} \int dE P_{\alpha\beta}^0(E, L) \int d\bar{E} |f(E, \bar{E})|^2 \phi_\alpha(\bar{E}) \sigma_\beta(\bar{E}) R(E_r, \bar{E}). \quad (2.16)$$

Next, we notice that, while $|f(E, \bar{E})|^2$ as a function of \bar{E} has a peak of small width σ_E at $\bar{E} = E$ or very close to this value, the flux $\phi_\alpha(\bar{E})$ and the cross section $\sigma_\beta(\bar{E})$ are smooth functions that change very little over the intervals $\Delta\bar{E} \sim \sigma_E$; therefore to a very good accuracy they can be replaced by their values at $\bar{E} = E$ and pulled out of the inner integral. This yields

$$N(E_r) = \mathcal{N} \int dE \phi_\alpha(E) P_{\alpha\beta}^0(E, L) \sigma_\beta(E) \tilde{R}(E_r, E), \quad (2.17)$$

where

$$\tilde{R}(E_r, E) = \int d\bar{E} R(E_r, \bar{E}) |f(E, \bar{E})|^2. \quad (2.18)$$

Comparing this result with (2.14), we see that they differ in two respects: first, the integrand of (2.17) contains the standard oscillation probability $P_{\alpha\beta}^0(E, L)$ (which is free from any decoherence effects) rather than the full probability $P_{\alpha\beta}(E, L)$ of eq. (2.1); second, (2.17) contains an effective energy resolution function $\tilde{R}(E_r, E)$ rather than the true one. This shows that effects of quantum decoherence due to WP separation can be incorporated into a modification of the energy resolution function of the detector and so are intimately entangled with it.

How much is the detector resolution modified by including the possible quantum decoherence effects into it? To illustrate this, we consider the case where both the energy-space neutrino WP and the resolution function $R(E_r, E)$ are of Gaussian form, that is, $|f(E, \bar{E})|^2$ is given by eq. (2.11) and²

$$R(E_r, \bar{E}) = \frac{1}{\sqrt{2\pi}\delta_E} e^{-\frac{(E_r - \bar{E})^2}{2\delta_E^2}}. \quad (2.19)$$

Substituting (2.11) and (2.19) into eq. (2.18) and extending the energy integration to the interval $(-\infty, \infty)$ (which is justified because the integrand has peaks of small width at positive values of \bar{E}), we obtain

$$\tilde{R}(E_r, E) = \frac{1}{\sqrt{2\pi(\delta_E^2 + \sigma_E^2)}} e^{-\frac{(E_r - E)^2}{2(\delta_E^2 + \sigma_E^2)}}. \quad (2.20)$$

For $\delta_E \gg \sigma_E$, the effective energy resolution function $\tilde{R}(E_r, E)$ essentially coincides with the true one. This means that in this case quantum decoherence by WP separation can be completely neglected, and whether or not the oscillations will be damped will be determined by condition (1.5). The separation of WPs may only be probed by the experiment if $\sigma_E \gtrsim \delta_E$.

2.3 Radioactive source experiments

In experiments of this type neutrinos are emitted by a β -radioactive source placed inside or near the detector. Usually, β -decay by electron capture is considered for the source; in

²Gaussian energy resolution functions with energy-dependent widths $\delta_E(E)$ are often used by experimentalists. Here for simplicity we take δ_E to be energy independent.

this case neutrinos have (quasi)monoenergetic spectra. By now, source experiments have been performed by the GALLEX [23, 24], SAGE [25, 26] and more recently BEST [15–17] collaborations. In all these cases ^{71}Ga was used as the target, and ^{71}Ge atoms produced as a result of neutrino capture by gallium were counted. Neutrino energy was not measured, and therefore, unlike in reactor experiments, the detection rates had no dependence on the neutrino energy resolution.³ GALLEX and SAGE measured the coordinate-averaged neutrino flux, whereas BEST comprises an inner and an outer targets and therefore has some coordinate sensitivity.

Consider a neutrino source experiment with e -capture radioactive nuclei as a source and counting of daughter nuclei as the means of neutrino detection. Experiments of this type look for ν_e disappearance and therefore the observed signal depends on $P_{ee}(E, L)$. We shall be assuming that the source is small compared with both the detector size and the neutrino oscillation length; the source can then be considered as pointlike. We shall put the origin of coordinates at the source. The detector may consist of one or more target volumes V_i . The number of events per unit time in the i th volume can then be written as

$$N_i(t) = n_0 \int_{V_i} d^3r \int d\bar{E} \phi_e(\bar{E}, r; t) \sigma_e(\bar{E}) P_{ee}(\bar{E}, r), \quad (2.21)$$

where n_0 is the number density of the target nuclei and

$$\phi_e(\bar{E}, r; t) = \frac{\Phi_e(\bar{E}, t)}{4\pi r^2} \quad (2.22)$$

is the flux of ν_e at the distance r from the source at the time t . The quantity $\Phi_e(\bar{E}, t)$ can be written as

$$\Phi_e(\bar{E}, t) = \Gamma_0 N(t) S(\bar{E}), \quad (2.23)$$

where Γ_0 is the electron capture rate of the source atoms, $N(t)$ is the number of the source atoms at the time t (which decreases with time following the exponential decay law) and $S(\bar{E})$ is the normalized spectrum of the produced neutrinos. It is characterized by a width δ_{El} which usually exceeds significantly the natural linewidth and is determined by a number of inhomogeneous broadening effects, such as Doppler broadening. Note that inhomogeneous broadening leads to the spread of the mean energies \bar{E} of the WPs of the emitted neutrinos due to the individual emitters being in slightly different conditions. We shall discuss inhomogeneous broadening (as well as homogeneous broadening which affects $f(E, \bar{E})$) in more detail in section 3.2 below.

We shall now follow essentially the same steps as in section 2.2. Using eqs. (2.22) and (2.23) in (2.21), we obtain

$$N_i(t) = n_0 \Gamma_0 N(t) \int_{V_i} \frac{d^3r}{4\pi r^2} \mathcal{F}(r), \quad (2.24)$$

³There have been suggestions to use neutrino-electron scattering rather than neutrino capture by atomic nuclei as a detection process in source experiments, see e.g. [27, 28]. In those cases the experimental energy resolution functions would have to be taken into account. With minor modifications, the formalism developed in section 2.2 would then apply.

where

$$\mathcal{F}(r) = \int d\bar{E} S(\bar{E}) \sigma_e(\bar{E}) P_{ee}(\bar{E}, r). \quad (2.25)$$

Let us consider the quantity $\mathcal{F}(r)$. Substituting in (2.25) the expression for $P_{ee}(\bar{E}, r)$ from (2.15) and changing the order of integrations over E and \bar{E} yields

$$\mathcal{F}(r) = \int dE P_{ee}^0(E, r) \int d\bar{E} S(\bar{E}) \sigma_e(\bar{E}) |f(E, \bar{E})|^2. \quad (2.26)$$

The cross section $\sigma_e(\bar{E})$ changes very little over the energy intervals $\Delta\bar{E} \sim \sigma_E$, and therefore it can be replaced by its value at $\bar{E} = E$ and pulled out of the inner integral in (2.26). This gives

$$\mathcal{F}(r) = \int dE P_{ee}^0(E, r) \sigma_e(E) \tilde{S}(E), \quad (2.27)$$

where

$$\tilde{S}(E) = \int d\bar{E} S(\bar{E}) |f(E, \bar{E})|^2. \quad (2.28)$$

All the effects of decoherence by WP separation are now incorporated into a modification of the neutrino spectrum $S(E)$, which is replaced by the effective spectrum $\tilde{S}(E)$. Note that for source experiments the effective spectrum $\tilde{S}(E)$ plays essentially the same role as the effective energy resolution $\tilde{R}(E_r, E)$ plays for reactor experiments (cf. eq. (2.18)).

Obviously, if the energy width σ_E of the neutrino WP satisfies $\sigma_E \ll \delta_{El}$, one can replace $S(\bar{E})$ by $S(E)$ in eq. (2.28) and pull it out of the integral, which gives $\tilde{S}(E) = S(E)$. Eqs. (2.24) and (2.27) then yield the usual expression for the event rate in the absence of WP decoherence. The damping will then only depend on the width of the neutrino spectrum δ_{El} .

In the opposite limit, $\sigma_E \gg \delta_{El}$, one can instead pull out of the integral the factor $|f(E, \bar{E})|^2$ at $\bar{E} = E_0$, where E_0 is the central energy of the neutrino spectrum. Eq. (2.28) then gives $\tilde{S}(E) = |f(E, E_0)|^2$. This yields

$$\mathcal{F}(r) = \int dE P_{ee}^0(E, r) \sigma_e(E) |f(E, E_0)|^2 \simeq \sigma_e(E_0) P_{ee}(E_0, r), \quad (2.29)$$

where we have used eq. (2.15). The oscillation probability $P_{ee}(E_0, r)$ here fully takes into account possible WP decoherence effects.

As before, we illustrate the above points by using the Gaussian form of the neutrino WP (2.11) and assuming that the spectrum of the neutrinos produced by the radioactive source is also Gaussian:

$$S(\bar{E}) = \frac{1}{\sqrt{2\pi}\delta_{El}} e^{-\frac{(\bar{E}-E_0)^2}{2\delta_{El}^2}}. \quad (2.30)$$

Eq. (2.28) then gives for the effective neutrino spectrum $\tilde{S}(E)$ the expression that coincides with the right-hand side of eq. (2.20) with the replacements $\delta_E \rightarrow \delta_{El}$, $E_r \rightarrow E_0$.

3 Lengths of neutrino wave packets

Let us now estimate the lengths of the neutrino WPs and the corresponding neutrino energy uncertainties σ_E for reactor and radioactive source experiments.

The length of the WP of a neutrino produced in a decay or collision process is given by [21, 22]

$$\sigma_x \simeq \frac{v_g - v_P}{\sigma_E}, \quad (3.1)$$

where v_g is the velocity of the emitted neutrino and v_P is the velocity of the neutrino source. For reactor and radioactive source experiments, the neutrino source is a highly non-relativistic nucleus and its velocity v_P can be neglected compared with $v_g \simeq 1$ in eq. (3.1). The QM uncertainty of neutrino energy σ_E is given by the inverse of the temporal duration of the production process σ_t : $\sigma_E \simeq \sigma_E^S = \sigma_t^{-1}$.⁴

We shall consider two cases:

- (i) Particles accompanying neutrino production are not detected and do not interact with the surrounding medium.
- (ii) Some or all of the particles accompanying neutrino production are “measured”, i.e. they are either directly detected or interact with the particles of the medium.

3.1 Wave packets of reactor (anti)neutrinos

Consider first neutrino emission in β -decays of nuclear fragments produced in fission reactions in nuclear reactors,

$$N \rightarrow N' + e^- + \bar{\nu}_e, \quad (3.2)$$

where N and N' are the parent and daughter nuclei.

3.1.1 Neutrino WPs in the case of delocalized accompanying particles

We start with the case when all the particles produced together with neutrino escape freely. In this case they do not affect the neutrino production time and the neutrino simply inherits the energy uncertainty of the parent unstable nucleus. If this nucleus is free or quasi-free, i.e. its interactions with the medium can be neglected, neutrino emission proceeds uninterrupted, and the characteristic emission time satisfies $\sigma_t \simeq \tau_N$, where τ_N is the mean lifetime of N . Thus, in this case $\sigma_E \simeq 1/\tau_N = \Gamma_N$, where Γ_N is the decay width of the parent nucleus.

If, however, N experiences collisions with the particles of the medium and the average time interval between two successive collisions is shorter than the lifetime τ_N , such interactions will lead to interruptions of coherent neutrino emission and therefore will increase its energy uncertainty σ_E . This effect is analogous to collisional broadening of photon emission lines in atomic physics. As we shall see, for neutrinos produced in β -decays of

⁴ As was discussed in section 2.1, the quantity σ_E of interest to us is actually the smaller between σ_E^S and σ_E^D which correspond, respectively, to neutrino production and detection. It can be shown that in the cases we consider this is actually σ_E^S , which we hereafter will simply denote σ_E .

fission products in nuclear reactors collisional broadening is an important effect that has to be taken into account.

We shall bear in mind that the duration of the processes of collision of the parent nucleus N with the surrounding particles of the medium are very short compared to its lifetime τ_N and shall also assume that these collisions introduce uncontrollable random phases into the wave function of the emitted neutrino state. In this approach (known in atomic physics as the Lorentz–Van Vleck–Weisskopf approach, see e.g. ref. [29]), the energy width of the WPs of the emitted neutrino state obeys

$$\sigma_E \simeq \sqrt{\Gamma_N^2 + 1/t_N^2}, \quad (3.3)$$

where t_N is the mean time interval between two successive collisions (mean free time).

Let us estimate t_N . Immediately after the fission the kinetic energies of the produced nuclear fragments can be as large as about 100 MeV. The fragments quickly thermalize on the time scale that is many orders of magnitude shorter than their lifetimes τ_N with respect to β -decay.⁵ Therefore, at the moment of the decay the parent nuclei are in thermal equilibrium with the medium, and their velocities are determined by the temperature of the medium T . For a fragment of mass m_N the average velocity is

$$v_N = \sqrt{\frac{3T}{m_N}}. \quad (3.4)$$

Taking for estimate $T \simeq 0.1$ eV (1160 K) and $m_N \simeq 100$ GeV, we find

$$v_N \simeq 1.7 \times 10^{-6} c \simeq 5.2 \times 10^4 \text{ cm/s}. \quad (3.5)$$

As the velocities of the fragments are small compared with the velocities of atomic electrons, they drag along the electrons of the parent atom of the fissile material and emerge as neutral or weakly ionized atoms. Their interactions with the medium are therefore described by atomic scattering cross sections σ_{AA} .

Nuclear fuel of commercial reactors is usually composed of a mixture of ^{235}U , ^{238}U , ^{239}Pu and ^{241}Pu . For definiteness, we shall consider the scattering of nuclear fragments in pure ^{235}U (this simplification will not affect our estimates significantly). The average time between two successive collisions is then

$$t_N \simeq \frac{1}{\sigma_{AA} n_U v_N}, \quad (3.6)$$

where $n_U = 4.9 \times 10^{22} \text{ cm}^{-3}$ is the number density of uranium atoms. The mean free path of N , which actually determines its localization in the medium, is

$$X_N = v_N t_N = \frac{1}{\sigma_{AA} n_U}. \quad (3.7)$$

We take the radius of uranium atoms to be equal to their van der Waals radius $r_{\text{vdW}} = 1.86 \times 10^{-8} \text{ cm}$. For a crude estimate of σ_{AA} , we approximate it by the geometrical cross

⁵For short-lived fission fragments, the lifetimes are typically in the range of minutes to days.

section: $\sigma_{AA} \simeq \pi(2r_{\text{vdW}})^2$. This is expected to be a reasonable approximation because (i) the nuclear momenta satisfy $p_N r_{\text{vdW}} \gg 1$, so that the WKB approximation applies, and (ii) when the atoms approach each other to distances $\lesssim 2r_{\text{vdW}}$ they experience strong repulsion with a potential U which exceeds significantly both the kinetic energy of N (~ 0.15 eV) and the quantity $1/(m_N r_{\text{vdW}}^2) \simeq 0.1$ eV, and therefore the approximation of scattering on a rigid sphere should apply. Eqs. (3.6) and (3.5) then give

$$t_N \simeq 9 \times 10^{-14} \text{ s}, \quad (3.8)$$

and $X_N \simeq 5 \times 10^{-9}$ cm. As t_N is much shorter than the lifetime of the decaying nucleus, eq. (3.3) yields

$$\sigma_E \simeq t_N^{-1} \simeq 7.2 \times 10^{-3} \text{ eV}. \quad (3.9)$$

From (3.1) we then find that in the limit when the particles accompanying neutrino production are completely delocalized

$$\sigma_x \simeq \frac{v_g}{\sigma_E} \simeq 2.8 \times 10^{-3} \text{ cm}. \quad (3.10)$$

Note that from eqs. (3.10), (3.9) and (3.7) it follows that the expression for σ_x can also be written as

$$\sigma_x \simeq X_N \frac{v_g}{v_N}. \quad (3.11)$$

That is, the length of the neutrino WP is given in this case by the mean free path of the parent nucleus magnified by a very large factor $v_g/v_N \simeq 6 \times 10^5$.

3.1.2 Effects of localization of the decay products

Let us now take into account the interactions of the decay products accompanying neutrino emission with medium. We shall first consider the interactions of the daughter nucleus N' .

Collisions of N' with the atoms of the medium localize it within the spatial region of the size $X_{N'}$, which can be estimated similarly to the localization of N (see eq. (3.7)), using the same geometrical atom-atom scattering cross section σ_{AA} .⁶ Thus, the mean free paths of the parent and daughter nuclei are of the same order of magnitude:

$$X_{N'} \simeq X_N \simeq 5 \times 10^{-9} \text{ cm}. \quad (3.12)$$

The collisions of N' with the surrounding atoms interrupt the process of its coherent emission. As N' is produced in the same β -decay process in which the neutrino is emitted, this will also affect the coherence time of neutrino production σ_t .

Let us estimate the velocity $v_{N'}$ with which the daughter nucleus N' is emitted. On average, the momenta of all the particles in the final state of the β -decay process (3.2) are roughly of the same order: $p_e \sim p_\nu \sim p_{N'}$. For the typical reactor neutrino energy $E \simeq 3$ MeV and $m_{N'} \sim 100$ GeV we find

$$v_{N'} = p_{N'}/m_{N'} \sim 3 \times 10^{-5} c \simeq 10^6 \text{ cm/s}. \quad (3.13)$$

⁶We assume here that the van der Waals radii of the fission fragments are of the same order of magnitude as that of uranium.

For the mean time between two successive collisions of N' we therefore obtain

$$t_{N'} = \frac{X_{N'}}{v_{N'}} \simeq 5 \times 10^{-15} \text{ s}. \quad (3.14)$$

Comparing this with (3.8), we find that $t_{N'}$ is about a factor of 20 smaller than t_N .

Let us now consider effects of interaction with the medium of the electron produced in decay (3.2). The main effect of scattering of β -electrons on atoms is the ionization of the latter. For electron kinetic energies E_e up to a few keV, the cross section of electron-impact ionization of uranium σ_{eU} can be found in [30]. Extrapolating it to MeV-scale energies basing on the results of ref. [31]), for electron energies $E_e \sim 3 \text{ MeV}$ we find $\sigma_{eU} \simeq 1 \times 10^{-18} \text{ cm}^2$. Therefore, for the mean free path of electrons we obtain $X_e = 1/(\sigma_{eU} n_U) \simeq 2 \times 10^{-5} \text{ cm}$, which is a factor of 4×10^3 larger than X_N and $X_{N'}$. On the other hand, for typical electron momenta $p_e \sim 3 \text{ MeV}$ their velocities are close to 1, and therefore the average time between two successive collisions of a β -decay electron is

$$t_e = X_e/v_e \simeq 7 \times 10^{-16} \text{ s}. \quad (3.15)$$

As the collisions of the parent nucleus N and of the decay products in reaction (3.2) with the surrounding atoms of the medium lead to interruptions of their coherent propagation or emission, the time of the coherent production of neutrino is determined by the shortest among the coherence times t_N , $t_{N'}$ and t_e considered above, which turns out to be t_e . Therefore, for the temporal duration of the neutrino production process we have $\sigma_t \simeq t_e \sim 7 \times 10^{-16} \text{ s}$. Correspondingly, for the energy uncertainty of the produced neutrino and the length of its WP we find

$$\sigma_E \simeq t_e^{-1} \simeq 1 \text{ eV}, \quad \sigma_x \simeq 2 \times 10^{-5} \text{ cm}. \quad (3.16)$$

It has been shown in [21, 22] that the temporal duration of the neutrino production process σ_t is given by the time of overlap of the WPs of all the particles involved in neutrino production. Our approach, based on the consideration of mean free times of the involved particles, is in accord with this result. Our treatment merely implies that we take the lengths the WPs of these particles to be given by their mean free paths, which in fact determine their spatial localization.

This can be illustrated by space-time diagrams showing neutrino production, propagation and detection processes as well as the propagation and interactions of the accompanying particles in the WP approach [9]. In Fig. 1 the propagation of the WPs of the particles is schematically represented by bands in the (t, x) plane. The vertical sections of the bands give the lengths of the WPs, whereas their slopes are determined by their group velocities. The brown rectangle corresponds to the WP of the parent nucleus ($v_N \simeq 0$). Due to their different group velocities, the WPs of the neutrino mass eigenstates (ν_1 and ν_2) diverge with time and traveled distance, and their overlap decreases. The horizontal sections of the bands corresponding to the produced N' and electron are given by their mean free times, $t_{N'}$ and t_e , respectively; their intersection with the band representing the parent nucleus N gives the space-time localization of the production process and, in

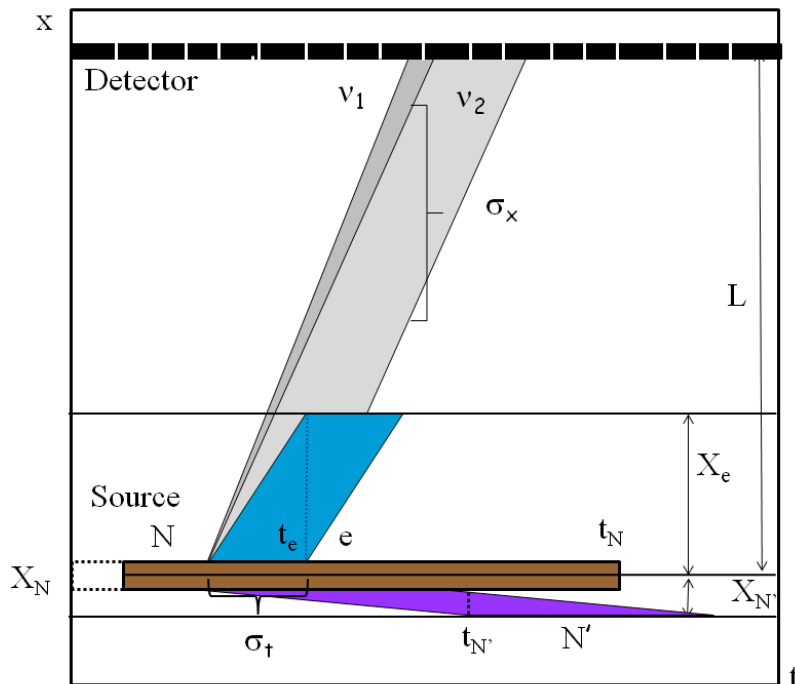


Figure 1. Schematic representation (space-time localization diagram) for neutrino production, propagation and detection in reactor experiments. Wave packets of the decaying nucleus N , daughter nucleus N' , electron and mass-eigenstate components of the emitted neutrino are represented by brown, violet, blue and gray bands, respectively. The slopes of the bands are determined by the group velocities of the particles. Black rectangles at $x = L$ show localization of the neutrino detection process. For simplicity, the WPs of only two neutrino mass eigenstates are shown.

particular, determines its duration σ_t . Thus, σ_t is given by the overlap time of the WPs of all the particles participating in neutrino production and is dominated by the WP of the particle with the shortest mean free time.

3.2 WP lengths and neutrino spectra in radioactive source experiments

Let us estimate the WP lengths σ_x and the spectra $S(\bar{E})$ of neutrinos in source experiments, taking experiments with radioactive ^{51}Cr as an example. Experiments with chromium source were carried out by GALLEX, SAGE and BEST collaborations.

As was mentioned in section 2.3, the shape and the width of the experimentally observed neutrino line are formed by two types of broadening effects – homogeneous and inhomogeneous broadening. Homogeneous broadening forms the line of each individual emitted neutrino of a given mean energy \bar{E} ; it includes such effects as natural linewidth, related to the finite lifetime of the parent atom, and collisional broadening due to the interaction of both the parent atom and of the particles accompanying neutrino production with the surrounding medium. These effects determine the width σ_E of the neutrino WP in energy representation $f(E, \bar{E})$ and the coordinate-space neutrino WP length $\sigma_x \simeq v_g/\sigma_E$. It is the homogeneous line broadening that may lead to decoherence by WP separation in

neutrino source experiments.

Inhomogeneous broadening is related to each individual neutrino emitter being in somewhat different conditions, like slightly different energies of atoms in a crystal due to crystal defects or velocity spread due to the thermal motion of the source atoms. This leads to emission of neutrinos with slightly different mean energies \bar{E} , i.e. it forms their spectrum $S(\bar{E})$ discussed in section 2.3. The spread of \bar{E} due to inhomogeneous broadening has nothing to do with decoherence by WP separation; however, as discussed above, averaging over the mean neutrino energies may also lead to observable damping of neutrino oscillations and thereby mimic quantum WP decoherence effects.

^{51}Cr decays via the electron capture process



with emission of four quasi-monoenergetic neutrino lines, grouped pairwise around 0.75 MeV (90%) and 0.43 MeV (10%), with the half-life time 27.7 d. For definiteness, we will consider emission of neutrinos with energy 0.75 MeV. For the electron capture process (3.17) the temporal duration σ_t of the neutrino production process will be given by the smaller between the mean free times of the the parent ^{51}Cr and the produced ^{51}V atoms.

We shall first consider homogeneous broadening effects. Chromium is a transition metal with *bcc* (body-centered cubic) crystalline structure and lattice constant 2.91×10^{-8} cm. As the localization length of the chromium atoms X_{Cr} , one can take the rms deviation of their positions from the equilibrium positions in the crystal due to thermal vibrations. Assuming the temperature of the chromium source $T \sim 600\text{K}$,⁷ we find $X_{\text{Cr}} \simeq 8.2 \times 10^{-9}$ cm [32]. For rms velocity of thermal vibrations of chromium atoms in the crystal lattice we find $v_{\text{Cr}} \simeq 1.7 \times 10^{-6}c$. This gives the mean free time of chromium atoms $t_{\text{Cr}} = X_{\text{Cr}}/v_{\text{Cr}} \simeq 1.6 \times 10^{-13}$ s.

Consider now the mean free time of vanadium atoms. From the kinematics of the decay it follows that the vanadium nuclei and the neutrinos produced in the decay process have equal momenta, $p_{\text{V}} = p_{\nu} = 0.75\text{ MeV}$. Therefore, the recoil energy and the velocity of the vanadium nucleus are $E_{\text{V}} \simeq 5.9\text{ eV}$ and $v_{\text{V}} \simeq 1.6 \cdot 10^{-5}c$, respectively. Because the recoil velocity of vanadium is small compared with the velocity of atomic electrons, vanadium emerges from the decay process in the form of neutral or weakly ionized atoms. The mean free path of the vanadium atoms in chromium can therefore be found as $X_{\text{V}} = (\sigma_{AA}n_{\text{Cr}})^{-1}$, where $n_{\text{Cr}} = 8.6 \times 10^{22}\text{ cm}^{-3}$ is the number density of chromium atoms and σ_{AA} is the cross section of V–Cr atomic scattering. The latter can be estimated as the geometrical cross section $\pi(r_{\text{vdW,Cr}} + r_{\text{vdW,V}})^2 \simeq 5.15 \times 10^{-15}\text{ cm}^2$, where we have used the numerical values of the van der Waals radii of chromium and vanadium $r_{\text{vdW,Cr}} = 2.00 \times 10^{-8}\text{ cm}$ and $r_{\text{vdW,V}} = 2.05 \times 10^{-8}\text{ cm}$. For the mean free path and mean free time of the vanadium atoms we then find $X_{\text{V}} = 2.26 \times 10^{-9}\text{ cm}$, $t_{\text{V}} = X_{\text{V}}/v_{\text{V}} \simeq 4.7 \times 10^{-15}\text{ s}$.

Because the mean free time of the vanadium atoms is much shorter than that of the chromium ones, the temporal duration of the neutrino production process is determined by the former: $\sigma_t \simeq t_{\text{V}} \simeq 4.7 \times 10^{-15}\text{ s}$. Correspondingly, for the energy width and the

⁷Note that the temperature of the source decreases with time during the experiment.

length of the neutrino WP we obtain

$$\sigma_E \simeq t_V^{-1} \simeq 0.14 \text{ eV}, \quad \sigma_x \simeq X_V \frac{v_g}{v_V} \simeq 1.4 \times 10^{-4} \text{ cm}. \quad (3.18)$$

Thus, the length of the neutrino WP is given by the mean free path of the vanadium atoms magnified by the factor $v_g/v_V \simeq 6.3 \times 10^4$. The contribution of the natural linewidth of ^{51}Cr to σ_E ($\Gamma_{\text{Cr}} \simeq 3.96 \times 10^{-22} \text{ eV}$) is completely negligible.

Consider now the distribution of the mean energies of the neutrino WPs, $S(\bar{E})$. As was mentioned above, there are several incoherent broadening effects that contribute to it, such as e.g. crystal defects and impurities; the largest contribution comes from Doppler broadening related to the fact that the source atoms are not at rest but experience thermal vibrations with the rms velocity v_{Cr} . Doppler broadening leads to the Gaussian shape of the line, as given in eq. (2.30). In the case under consideration the corresponding width is

$$\delta_{El} = \frac{v_{\text{Cr}}}{c} E_0 \simeq 1.3 \text{ eV}, \quad (3.19)$$

where we have used $E_0 = 0.75 \text{ MeV}$ for the central energy of the line. Thus, the width of the energy spectrum of the ^{51}Cr line δ_{El} exceeds the energy uncertainty σ_E of the neutrino WPs by an order of magnitude.

Effect of localization of the accompanying particles (N' from e -capture, e and N' from β -decay) on the neutrino WP length can be estimated in different way: Instead of the mean free paths of the accompanying particles one can consider the temporal durations of processes of their interactions with particles of medium σ_t^i ($i = e, N'$). Velocities of the accompanying particles v_i and σ_t^i allow to construct the corresponding WP bands. Then the neutrino WPs will be determined by intersection of these bands and the band of original nuclei N . For $\sigma_t^i \ll t_N$, the size of neutrino WP will be substantially reduced in comparison to the case when interactions of the accompanying particles are neglected.

In turn, σ_t^i are determined by WPs of atoms of medium and WPs of products of secondary particle interactions. The problem is that one should consider the chain of interactions which probably ends up by thermalization of the products.

In the case of e -capture the WP size of produced Vanadium is determined by the duration of the process $^{51}\text{V} + ^{51}\text{Cr} \rightarrow ^{51}\text{V}' + ^{51}\text{Cr}'$, σ_{Cr} . To find σ_{Cr} , apart from localization of ^{51}Cr , one should know the WPs of $^{51}\text{V}'$ and $^{51}\text{Cr}'$, etc. The estimation show that the chain of secondary interactions can reduce σ_{Cr} by factor $10^{-2} - 10^{-1}$ in comparison to t_{Cr} . This gives the length of neutrino WP, σ_x , of the same order as in (3.18).

A note on the detection processes is in order. As was pointed out above (see footnote 4), our estimates show that for reactor and source experiments energy uncertainties inherent to neutrino detection are much larger than those inherent to neutrino production, $\sigma_E^D \gg \sigma_E^S$, so that to a very good accuracy $\sigma_E = \sigma_E^S$. The condition $\sigma_E^D \gg \sigma_E^S$ allows one to replace $f_D(E)$ in eq. (2.3) by a constant; this means that in the cases under consideration the detection processes do not affect neutrino coherence. For this reason we did not consider them in detail.

4 Discussion

We have shown that the effects of decoherence by WP separation can always be incorporated into a modification of the detector resolution function or, for source experiments, of the shape and width of the neutrino line; therefore, these two sources of the oscillation damping are equivalent from the observational point of view. Note that in the case of Gaussian averaging, the observational equivalence of WP decoherence and averaging over L/E was previously shown in [7].

We have found that the effective detector energy resolution functions (or effective widths of the neutrino line) are always dominated by the larger between the inherent QM uncertainty of neutrino energy σ_E and the detector resolution δ_E (or the linewidth δ_{El}). For Gaussian WPs and resolution functions, the effective resolution is characterized by

$$\delta_{E\text{eff}} = \sqrt{\delta_E^2 + \sigma_E^2}, \quad (4.1)$$

and similarly for the effective neutrino linewidth $\delta_{El\text{eff}}$ for the source experiments. It should be stressed that in the latter case the width of the neutrino spectrum $S(\bar{E})$ is dominated by Doppler broadening, which does lead to $S(\bar{E})$ of Gaussian form.

Our results show that for reactor neutrinos the effects of WP separation may only be experimentally probed if $\sigma_E > \delta_E$ (for radioactive source experiments the corresponding condition is $\sigma_E > \delta_{El}$). This has to be complemented by a condition on the baseline of the experiment L , which will be discussed below.⁸

For reactor experiments, our estimates gave for the lengths of the neutrino WPs and the corresponding QM neutrino energy uncertainties

$$\sigma_x \simeq 2 \times 10^{-5} \text{ cm}, \quad \sigma_E \simeq 1 \text{ eV}. \quad (4.2)$$

The latter value has to be compared with detector energy resolution in reactor experiments. Currently, it is in the sub-MeV region; the forthcoming JUNO experiment aims at a very high energy resolution of about 3%, which corresponds to $\delta_E \sim 100 \text{ keV}$. Eq. (4.2) then gives $\sigma_E/\delta_E \sim 10^{-5}$, which means that effects of oscillation damping by WP separation cannot be seen in reactor neutrino experiments. This also means that these WP-related quantum decoherence effects cannot hinder the determination of the neutrino mass ordering, which is one of the major goals of JUNO.

Our estimate of the WP lengths of reactor neutrinos in eq. (4.2) can also be compared with the lower bound (1.1) obtained from the combined analysis of the existing reactor neutrino data in [2, 3]; our result exceeds this lower limit by six orders of magnitude.

For the WP lengths and intrinsic energy uncertainties of neutrinos in chromium radioactive source experiments we found

$$\sigma_x \simeq 1.4 \times 10^{-4} \text{ cm}, \quad \sigma_E \simeq 0.14 \text{ eV}. \quad (4.3)$$

⁸From eq. (2.20) one could conclude that WP separation effects may be observable even if the condition $\sigma_E \gtrsim \delta_E$ is not met, provided that the energy resolution of the detector is known with very high accuracy, so that its error $\Delta(\delta_E)$ is smaller than σ_E . However, as follows from (2.20), this would require unrealistically high accuracy of the detector resolution function, $\Delta(\delta_E) \sim \sigma_E^2/\delta_E^2$; more importantly, as we shall see, even perfectly known energy resolution of the detector would not allow one to observe WP separation effects because of the constraints on the baseline L .

These values differ from the corresponding values for reactor neutrinos by roughly one order of magnitude. The value of σ_E in eq. (4.3) is about a factor of ten smaller than the energy width of the detected neutrino line, $\delta_{El} \simeq 1.3$ eV. We see that the disparity between the QM neutrino energy uncertainty and the energy resolution of the experiment is in this case much weaker than it is for reactor experiments.

As was pointed out in the Introduction, in ref. [5] an attempt had been made to reconcile the results of short-baseline reactor experiments and the radioactive source experiment BEST basing on the WP nature of neutrinos. The value of the neutrino WP length σ_x was chosen to be equal to the lower bound (1.1) found in [2, 3]. However, according to our estimates, this lower bound is orders of magnitude below the actual values of σ_x for both reactor and chromium-source neutrinos. Therefore, WP separation effects cannot reconcile the results of the reactor and BEST experiments.

Can one still contemplate a terrestrial experiment that would be sensitive to the size of the neutrino WP? As σ_E/δ_{El} is relatively large for ^{51}Cr source experiments, one could think about source experiments with smaller δ_{El} , e.g. look for radioactive sources with smaller neutrino energy E_0 . This would reduce the Doppler broadening of the neutrino line, which is proportional to E_0 (see eq. (3.19)). However, decreasing E_0 would also mean that the recoil momenta of the daughter nuclei produced in the electron capture process would decrease. As follows from the discussion in section 3.2, this would also decrease σ_E ; as a result, the ratio σ_E/δ_{El} will be unaffected.

A more practical option would probably be to cool down the source. This would suppress Doppler broadening effects without decreasing σ_E . In any case, for radioactive source experiments the values of σ_E and δ_{El} are not very different, does that mean that one could probe decoherence by WP separation in such experiments?

The answer seems to be negative. The point is that although the requirement $\sigma_E \gtrsim \delta_E$ (or $\sigma_E \gtrsim \delta_{El}$) is a necessary condition for observability of WP separation effects, it is not sufficient. Irrespectively of whether σ_E is smaller or larger than δ_E (or δ_{El}), for the WP separation effects to develop neutrinos should travel sufficiently large distances, comparable to or larger than the coherence length. For reactor neutrino experiments, from eq. (4.2) and the definition of the coherence length in eq. (2.8) we find

$$L_{\text{coh},21} \simeq 4.8 \times 10^7 \text{ km}, \quad L_{\text{coh},31} \simeq 1.4 \times 10^6 \text{ km}, \quad L_{\text{coh},41} \simeq 3600 \text{ km}. \quad (4.4)$$

Here $L_{\text{coh},21}$ and $L_{\text{coh},31}$ correspond to neutrino mass square differences $\Delta m_{12}^2 \simeq 7.5 \times 10^{-5} \text{ eV}^2$ and $\Delta m_{31}^2 \simeq 2.5 \times 10^{-3} \text{ eV}^2$, respectively, and $L_{\text{coh},41}$ corresponds to much discussed hypothetical active-sterile neutrino oscillations with $\Delta m_{41}^2 \simeq 1 \text{ eV}^2$. Neutrino energy $E = 3 \text{ MeV}$ was assumed. For the chromium source experiment ($E = 0.75 \text{ MeV}$), the value of σ_x from eq. (4.3) yields

$$L_{\text{coh},21} \simeq 2.1 \times 10^7 \text{ km}, \quad L_{\text{coh},31} \simeq 6.3 \times 10^5 \text{ km}, \quad L_{\text{coh},41} \simeq 1600 \text{ km}. \quad (4.5)$$

Obviously, no reactor or neutrino source experiments with such baselines are possible.

The coherence lengths are inversely proportional to Δm_{ik}^2 , and one could therefore expect that it is easier to probe the effects of decoherence by WP separation in experiments that are sensitive to larger mass square differences, such as active-sterile neutrino

oscillations experiments [5]. This is, however, misleading. The point is that experiments are usually devised such that the experimental baseline is of the order of the expected neutrino oscillation length. As the latter is also inversely proportional to Δm_{ik}^2 , the ratio

$$\frac{L_{\text{coh},ik}}{l_{\text{osc},ik}} = \frac{\sigma_x E}{2\pi} \quad (4.6)$$

is independent of Δm_{ik}^2 . Note that this quantity is Lorentz-invariant, as so is $\sigma_x E$ [33]. For reactor experiments we find $L_{\text{coh}}/l_{\text{osc}} \sim 5 \times 10^5$, that is, decoherence by WP separation would have started to be seen only after neutrinos have propagated half a million oscillation lengths. Similar estimate holds for neutrino source experiments. This is by far much larger than any reasonable baseline in terrestrial neutrino experiments. Obviously, even if experiments with such huge L were possible, effects of averaging due to finite energy resolution of the detectors would reveal themselves much before. From eq. (4.6) it follows that the WP separation effects should become more pronounced with decreasing E ; it is however not easy to detect neutrinos with energies much below the MeV range.

We conclude that it is not possible to observe effects of quantum decoherence by WP separation in terrestrial neutrino experiments, at least for the class of experiments we considered (i.e. reactor and radioactive neutrino source experiments). If a damping of the oscillations which exceeds the expected damping related to the usual averaging due to the (accurately known) finite energy resolution of the detector, or due to the finite neutrino linewidth in source experiments, is nevertheless observed, this will signify some new physics and not decoherence by WP separation.

Acknowledgement. We thank D. Gorbunov for useful correspondence.

References

- [1] F. P. An *et al.* [Daya Bay], “Study of the wave packet treatment of neutrino oscillation at Daya Bay,” *Eur. Phys. J. C* **77** (2017) no.9, 606 [arXiv:1608.01661 [hep-ex]].
- [2] A. de Gouvea, V. de Romeri and C. A. Ternes, “Probing neutrino quantum decoherence at reactor experiments,” *JHEP* **08** (2020), 018 [arXiv:2005.03022 [hep-ph]].
- [3] A. de Gouvêa, V. De Romeri and C. A. Ternes, “Combined analysis of neutrino decoherence at reactor experiments,” *JHEP* **06** (2021), 042 [arXiv:2104.05806 [hep-ph]].
- [4] J. Wang *et al.* [JUNO], “Damping signatures at JUNO, a medium-baseline reactor neutrino oscillation experiment,” *JHEP* **06** (2022), 062 [arXiv:2112.14450 [hep-ex]].
- [5] C. A. Argüelles, T. Bertólez-Martínez and J. Salvado, “Impact of wave packet separation in low-energy sterile neutrino searches,” [arXiv:2201.05108 [hep-ph]].
- [6] M. Blennow, T. Ohlsson and W. Winter, “Damping signatures in future neutrino oscillation experiments,” *JHEP* **06** (2005), 049 [arXiv:hep-ph/0502147 [hep-ph]].
- [7] T. Ohlsson, “Equivalence between neutrino oscillations and neutrino decoherence,” *Phys. Lett. B* **502** (2001), 159-166 [arXiv:hep-ph/0012272 [hep-ph]].
- [8] B. Kayser and J. Kopp, “Testing the wave packet approach to neutrino oscillations in future experiments,” [arXiv:1005.4081 [hep-ph]].

- [9] E. Akhmedov, D. Hernandez and A. Smirnov, “Neutrino production coherence and oscillation experiments,” *JHEP* **04** (2012), 052 [arXiv:1201.4128 [hep-ph]].
- [10] B. J. P. Jones, “Dynamical pion collapse and the coherence of conventional neutrino beams”, *Phys.Rev.* **D 91** (2015) 5, 053002 [arXiv: 1412.2264 [hep-ph]]
- [11] P. Coloma, J. Lopez-Pavon, I. Martinez-Soler and H. Nunokawa, “Decoherence in neutrino propagation through matter, and bounds from IceCube/DeepCore,” *Eur. Phys. J. C* **78** (2018) no.8, 614 [arXiv:1803.04438 [hep-ph]].
- [12] J. A. B. Coelho, W. A. Mann and S. S. Bashar, “Nonmaximal θ_{23} mixing at NOvA from neutrino decoherence,” *Phys. Rev. Lett.* **118** (2017) no.22, 221801 [arXiv:1702.04738 [hep-ph]].
- [13] G. Balieiro Gomes, D. V. Forero, M. M. Guzzo, P. C. De Holanda and R. L. N. Oliveira, “Quantum decoherence effects in neutrino oscillations at DUNE,” *Phys. Rev. D* **100** (2019) no.5, 055023 [arXiv:1805.09818 [hep-ph]].
- [14] V. A. Naumov and D. S. Shkirmanov, “Reactor antineutrino anomaly reanalysis in context of inverse-square law violation,” *Universe* **7** (2021) no.7, 246
- [15] V. V. Barinov, *et al.* “Results from the Baksan Experiment on Sterile Transitions (BEST),” [arXiv:2109.11482 [nucl-ex]].
- [16] V. Barinov and D. Gorbunov, “BEST Impact on sterile neutrino hypothesis,” [arXiv:2109.14654 [hep-ph]].
- [17] V. V. Barinov *et al.*, “A Search for electron neutrino transitions to sterile states in the BEST experiment,” [arXiv:2201.07364 [nucl-ex]].
- [18] B. Kayser, “On the quantum mechanics of neutrino oscillation,” *Phys. Rev. D* **24** (1981) 110.
- [19] E. K. Akhmedov and A. Y. Smirnov, “Paradoxes of neutrino oscillations,” *Phys. Atom. Nucl.* **72** (2009), 1363-1381 [arXiv:0905.1903 [hep-ph]].
- [20] C. Giunti and C. W. Kim, “Coherence of neutrino oscillations in the wave packet approach,” *Phys. Rev. D* **58** (1998), 017301 [arXiv:hep-ph/9711363 [hep-ph]].
- [21] C. Giunti, “Neutrino wave packets in quantum field theory,” *JHEP* **11** (2002), 017 [arXiv:hep-ph/0205014 [hep-ph]].
- [22] M. Beuthe, “Oscillations of neutrinos and mesons in quantum field theory,” *Phys. Rept.* **375** (2003), 105-218 [arXiv:hep-ph/0109119 [hep-ph]].
- [23] W. Hampel *et al.* [GALLEX], “Final results of the Cr-51 neutrino source experiments in GALLEX,” *Phys. Lett. B* **420** (1998), 114-126
- [24] F. Kaether, W. Hampel, G. Heusser, J. Kiko and T. Kirsten, “Reanalysis of the GALLEX solar neutrino flux and source experiments,” *Phys. Lett. B* **685** (2010), 47-54 [arXiv:1001.2731 [hep-ex]].
- [25] J. N. Abdurashitov *et al.* [SAGE], “Measurement of the response of the Russian-American gallium experiment to neutrinos from a Cr-51 source,” *Phys. Rev. C* **59** (1999), 2246-2263 [arXiv:hep-ph/9803418 [hep-ph]].
- [26] J. N. Abdurashitov *et al.* [SAGE], “Measurement of the response of a Ga solar neutrino experiment to neutrinos from an Ar-37 source,” *Phys. Rev. C* **73** (2006), 045805 [arXiv:nucl-ex/0512041 [nucl-ex]].
- [27] J. D. Vergados, Y. Giomataris and Y. N. Novikov, “Novel way to search for sterile neutrinos,” *Phys. Rev. D* **85** (2012), 033003 [arXiv:1105.3654 [hep-ph]].

- [28] G. Bellini *et al.* [Borexino], “SOX: Short distance neutrino Oscillations with BoreXino,” *JHEP* **08** (2013), 038 [arXiv:1304.7721 [physics.ins-det]].
- [29] R. W. Parsons, V. I. Metchnik and R. J. Dyne, “The collision broadening of spectral lines”, *Aust. J. Phys.* **21** (1968) 13-20.
- [30] B. Goswami, R. Naghma and B. Antony, “Calculation of electron impact total ionization cross sections for tungsten, uranium and their oxide radicals”, *Int. J. Mass Spectrometry* **372** (2014) 8.
- [31] H. Gümüş, “Simple stopping power formula for low and intermediate energy electrons”, *Radiation Physics and Chemistry* **72** (2005) 7.
- [32] J. Trampenau, W. Petry and C. Herzig, “Temperature dependence of the lattice dynamics of chromium”, *Phys. Rev. B* **47** (1993) 3132.
- [33] Y. Farzan and A. Y. Smirnov, “Coherence and oscillations of cosmic neutrinos,” *Nucl. Phys. B* **805** (2008), 356-376 [arXiv:0803.0495 [hep-ph]].